Magar, K. (2025). Inspecting gaseous pollutants and their dynamics in Kathmandu using satellite derived data. *GeoFocus*, *Revista Internacional de Ciencia y Tecnología de la Información Geográfica* (Articles), 36, 43-62. https://dx.doi.org/10.21138/GF.835

INSPECTING GASEOUS POLLUTANTS AND THEIR DYNAMICS IN KATHMANDU USING SATELLITE DERIVED DATA

Keshab Magar
ksabmagar7@gmail.com

ABSTRACT

Air pollution is mostly due to anthropogenic causes degrading the quality of breathable air. The larger dimensions of gaseous pollutants are still challenging to inspect. Satellite data can quantify the concentrations of atmospheric pollutants that are specifically beneficial in understanding air pollution. This paper attempts to understand the air pollutants in the Kathmandu district (Nepal) retrieved from the Sentinel-5P satellite data from 2019 to 2022: by correlating with the weather parameter and vegetation indices, observing the yearly concentrations of the gaseous pollutants over the days of the year and observing their spatial distribution. In the results, temperature showed a predominantly strong positive correlation with methane (CH_4), carbon monoxide (CO) and ozone (O_3) and a negative correlation with nitrogen dioxide (NO_2), formaldehyde (HCHO), sulphur dioxide (SO_2) and aerosol. Precipitation was negatively correlated with all the pollutants except the O_3. Vegetation indices, Normalised Difference Vegetation Index (NDVI) and Enhanced Vegetation Index (EVI), were negatively correlated with most of the gaseous pollutants signifying the importance of the vegetation towards mitigating the gaseous pollutants. Moreover, yearly trends of the gaseous pollutants and the spatial distributions were unique for all the gaseous pollutants. Lowest mean concentrations of the aerosol index, HCHO, NO_2 and O_3 in different days of 2020 were suggestive towards the impacts of COVID-19 lockdown. In the broader context, proper vegetation and the remedial ways to maintain Kathmandu's temperature, around the city areas, is likely to moderate the gaseous pollutants in the city. This paper clearly points to the approach in utilising the satellite based data in air pollution inspections.

Keywords: air pollution; Sentinel-5P; TROPOMI; gaseous pollutants, remote sensing.

INSPECCIÓN DE CONTAMINANTES GASEOSOS Y SU DINÁMICA EN KATMANDÚ UTILIZANDO DATOS DERIVADOS DE SATÉLITES

RESUMEN

La contaminación del aire se debe principalmente a causas antropogénicas que degradan la calidad del aire respirable. Las dimensiones más grandes de los contaminantes gaseosos siguen siendo difíciles de inspeccionar. Los datos satelitales pueden cuantificar las concentraciones de contaminantes

Received: 28/10/2023 Accepted: 18/11/2025
Academic Editor: Dr. Ismael Vallejo www.geofocus.org

atmosféricos que son específicamente beneficiosos para comprender la contaminación del aire. Este artículo intenta comprender los contaminantes del aire en el distrito de Katmandú (Nepal) recuperados de los datos del satélite Sentinel-5P de 2019 a 2022: correlacionando con datos meteorológicos e índices de vegetación, observando las concentraciones anuales de los contaminantes gaseosos a lo largo de los días de los años y observando su distribución espacial. En los resultados, la temperatura mostró predominantemente una fuerte correlación positiva con metano (CH_4), monóxido de carbono (CO) y ozono(O_3), y una correlación negativa con dióxido de nitrógeno (NO_2), formaldehído (HCHO), dióxido de azufre (SO_2) y aerosol. La precipitación se correlacionó negativamente con todos los contaminantes excepto el O_3. Los índices de vegetación, Índice de Vegetación de Diferencia Normalizada (NDVI) e Índice de Vegetación Mejorado (EVI), se correlacionaron negativamente con la mayoría de los contaminantes gaseosos, lo que indica la importancia de la vegetación para mitigar los contaminantes gaseosos. Además, las tendencias anuales de los contaminantes gaseosos y las distribuciones espaciales fueron únicas para todos los contaminantes gaseosos. Las concentraciones medias más bajas del índice de aerosoles, HCHO, NO_2 y O_3 en diferentes días de 2020 sugirieron los impactos del confinamiento por COVID-19. En el contexto más amplio, es probable que la vegetación adecuada y las formas correctivas de mantener la temperatura de Katmandú, alrededor de las áreas de la ciudad, moderen los contaminantes gaseosos en la ciudad. Esta investigación señala claramente el enfoque en la utilización de datos basados en satélites en inspecciones de contaminación del aire.

Palabras clave: contaminación atmosférica; Sentinel-5P; TROPOMI; contaminantes gaseosos; teledetección.

1. Introduction

Air pollution is the qualitative degradation of the air by the physical, chemical, and biological causal factors that negatively impact human health (WHO 2023). Major air pollutants include different gaseous compounds such as carbon monoxide (CO), sulphur dioxide (SO_2), nitrogen oxides (NOx), ozone (O_3), heavy metals, and particulate matter whose sources are most often attributed to fossil fuels combustion or mostly anthropogenic causes in urban areas (Kampa and Castanas 2008). Exposure to polluted air has been associated with respiratory diseases, such as asthma and chronic obstructive pulmonary disease (COPD), which similarly disrupts the broad immune system and results in detrimental cellular mechanisms (Bernstein *et al.* 2004, Glencross *et al.* 2020). Along with respiratory health, polluted air negatively affects cardiac health due to oxidative stress when the cellular metabolism is ineffective in immunising against the pathogens (Fuertes *et al.* 2020).

In 2019, almost all of the world's population lived in areas where recommendations of air quality guidelines from World Health Organization (WHO) did not meet such as exceeding the limit of particulate matter of 10 micrograms per cubic metre. 7.8 % of global deaths are related to open-air pollution open-air pollution, while this is 10 % or more for some countries with older populations always at higher risk (Ritchie and Roser 2019). The global deaths from outside air pollution are increasing which is also due to population growth and ageing population but the air pollution still remains the major cause for the greatest number of deaths causing more than six million deaths in 2019 (Fuller *et al.* 2022). Likewise, outdoor air pollution has been estimated to have resulted in 4.2 million premature deaths that were mostly in low and middle-income countries of Southeast Asia and Western Pacific regions (WHO 2019).

Understandably, suggestive approaches to air pollution monitoring are in the preparation of air quality management plans specific to the location (Gulia *et al.* 2015). Improvements in the city structure with more green innovation, upgrades in the industrial sectors and decentralisations of the urban areas are likely to be decisive in improving air quality (Gao and Yuan 2022). Installing air quality monitors are equally advantageous in monitoring and assessing urban air quality and in some cases in determining the trends of air pollution, for instance annual NO_2 concentrations in 71 % of cities has increased at 0.4 % and ozone levels in 89 % of cities at 0.8 % annually (Sicard *et al.* 2023).

Challenges remain in air quality monitoring as the based ground-based sensors are sparse, and it can be expensive for the instalment of such sensors relative to the local region. The data generated

from the ground sensors require a representative area not influenced by the major air polluters. Although not replacive of the ground sensors, satellite-based data-based air quality monitoring has been heavily used in monitoring particulate matter and NO_2 at a surface level due to their more extensive spatial coverage and ability to unfold the daily changes to changes over the decades (Holloway *et al.* 2021). While influences from the atmospheric conditions are common, satellite data are still useful for areas when there are no ground-based sensors and multiple satellite-based sensors have been enormously utilised for estimating the air pollutants and monitoring the long term trend of concentrations (AbdelSattar 2019).

Sentinel-5P or Sentinel 5 Precursor (S5-P), launched on 13 October 2017, equipped with TROPOspheric Monitoring Instrument (TROPOMI) sensor, is the EU satellite for air pollution monitoring (ESA n.d.). Sentinel-5P generated data has been frequently used to study the spatial variation of air pollutants such as: observation of NO_2 concentrations in China during winter and summer seasons, and spatial distribution of the concentrations (Zheng *et al.* 2019), the spatial distribution of NO_2 over Europe during Covid-19 (Vîrghileanu *et al.* 2020), observation of NO_2 with the population in Turkey suggesting the study of other factors for air pollution (Kaplan *et al.* 2019), relating CO and NO_2 with population, altitude and vegetation (Kaplan and Avdan 2020), observing visible spatial patterns of NO_2 even in cleaner cities of Norway (Schneider *et al.* 2021) and evaluating CO and CH_4 during fire events in Portugal (Magro *et al.* 2021). Major objectives of the Sentinel-5P data have been the environmental monitoring attempts in quantifying the gaseous concentrations effectively (Bodah *et al.* 2022; Trenchev *et al.* 2023).

This study, in the series of using Sentinel-5P in air pollution monitoring, is an attempt to utilise the Sentinel-5P products for the Kathmandu district of Nepal. Although observations have been done in other parts of the world, satellite-based air pollution monitoring studies are limited in Nepal. Urbanisation, increased infrastructure activities and vehicular sources are the main reasons for the air pollution in Kathmandu deteriorating air quality and directly risking human health (Saud & Paudel, 2018). Due to the rapid and unplanned urbanisation, Kathmandu has seen major environmental challenges in all forms of pollution (Thapa *et al.* 2008). As the capital and most urbanised city of Nepal, it demands the need for satellite-based observation for air pollution monitoring.

The paper relates the Sentinel-5P data to the temperature, vegetation and rainfall data uniquely suggesting how the impacts on the gaseous pollutants are from those external factors. Understanding the role of these external factors as the dynamics would assist in developing effective mitigation strategies for reducing air pollution. In addition, observation of the time series of the air pollutants and the spatial patterns of the gaseous pollutants are necessary to provide valuable insights into the pollutants. The main objectives of this study are to observe the relation of the weather parameters (temperature, precipitation) and vegetation indices to the concentrations of gaseous pollutants (NO_2, CO, HCHO, SO_2, CH_4, O_3 and aerosol) retrieved from Sentinel-5P offline products. Yearly trends of the gaseous pollutants within the different days of year and spatial distribution of the gaseous pollutants over the Kathmandu district were observed.

2. Materials, data and methods

2.1. Study Area

Kathmandu, one of the 77 districts of Nepal, is the most populous district, which consists of the Kathmandu Metropolitan City or Kathmandu as the capital city of Nepal. Located from 27°27′E to 27°49′E longitude and 85°10′N to 85°32′N latitude, the district covers an area of 413.7 km^2 with a population of 2.017 million in 2021. Kathmandu district (Figure 1) is one of the three districts of the Kathmandu Valley, along with Lalitpur and Bhaktapur District. The altitude is roughly around 1200 m to 2700 m above sea level and mostly has a subtropical climate receiving 150 ml of annual rainfall. Kathmandu is surrounded by mountain ranges, which influence the microclimatic conditions. Although difficulties exist to classify Koppen-Geiger scheme based climate classification, the identifiable climate for Nepal, including the study area can be referred as temperate with dry winter and hot summer (Cwa) (Karki *et al.* 2016).

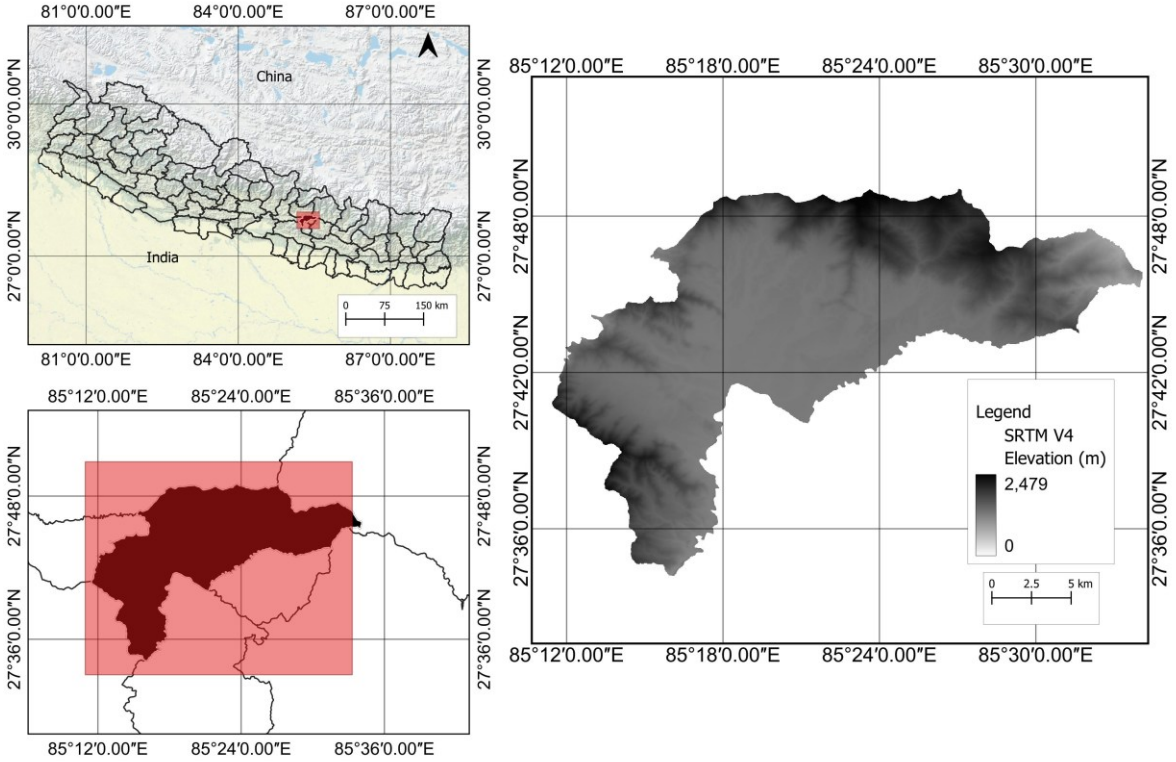

Figure 1. Location map of the study area

2.2. Data

2.2.1 Sentinel-5P

Tropospheric Monitoring Instrument (TROPOMI), onboard Sentinel-5P (S5-P), provides high-resolution data on various atmospheric parameters, mainly on gaseous constituents (ESA, n.d.-a). TROPOMI operates in the UV-SWIR (Ultraviolet to Short-Wave Infrared) wavelength range, each covering a specific wavelength range of 0.25 to 0.5 nm with 4 spectrometer bands (Vries *et al.* 2016).

These are available daily with global coverage with two versions: Near Real-Time (NRTI) and Offline (OFFL). The data include Sentinel-5P Offline products: Offline UV Aerosol Index, Offline Carbon Monoxide (CO), Offline Formaldehyde (HCHO), Offline Nitrogen Dioxide (NO_2), Offline Ozone (O_3), Offline Sulphur Dioxide (SO_2), Offline Methane (CH_4) and Offline UV Aerosol Layer Height which were used for the study. These are available after the latter half of the year 2018 except methane which is available from 2019 (only for the offline version).

The bands used for the study were "column volume mixing ratio dry air" for CH_4, "column number density" for other gaseous pollutants, "absorbing aerosol index" for aerosol index and "aerosol height" for aerosol layer height. For gaseous concentration, the measurements are performed for the concentrations of the gases along a vertical column that extends from the Earth's surface to the top of the atmosphere. Absorbing aerosol index refers to the presence of the UV-absorbing aerosols like dust and smoke and aerosol height means the altitude at which aerosol layers are located. The provided units of the gaseous concentrations are in mol/m^2, metre for aerosol height, unit less for aerosol index, and the unit for CH_4 is mol fraction. For CH_4, there are data gaps or missing data, for instance from 2022-07-26 and 2022-08-31, due to power outages and are missing for the study area as well.

All S5-P data are under Copernicus Sentinel Data Terms and Conditions, S5-P data are freely and fully available to all the users.

2.2.2 MODIS

Moderate Resolution Imaging Spectroradiometer (MODIS), on board Terra and Aqua satellites, was used for vegetation indices and temperature data. Vegetation indices utilise visible and near-infrared bands to provide the measure of vegetation ranging from -1 to +1. Higher values indicate the dense presence of the vegetation while the lower values mean the absence or scarceness of the vegetation. MODIS Land Surface Temperature (LST) products estimate the temperature of the Earth's land surface representing the Earth's uppermost layer and are available for both daytime and nighttime LST. Daily available Terra Land Surface Temperature for daytime and nighttime (MOD11A1.061) from Wan *et al.* (2021) of 1 km, Normalised Difference Vegetation Index (NDVI) and Enhanced Vegetation Index (EVI) of 500 m were used generated from the MODIS/006/MOD09GA surface reflectance composites (Vermote & Wolfe 2021).

Vegetation indices are used for study of various purposes and can be combined with data of other sensors, and the long-term availability of MODIS data have been used extensively (Huete *et al.* 2011). Furthermore, MODIS LST data have been used as well for varying applications (Phan & Kappas 2018).

2.2.3 CHIRPS

Climate Hazards Group InfraRed Precipitation With Station Data (CHIRPS) was used for the precipitation data. It is prepared with satellite imagery incorporated with in situ station data to create a gridded rainfall time series which is available for more than 30+ years starting from 1981 (Funk *et al.* 2015). CHIRPS has aspatial resolution of approximately 5 km by 5 km and is available daily or pentadal precipitation estimates. CHIRPS data has good correlation with recorded rainfall, mainly in the rainy season, especially in the rainy season and can be used as a substitute of the rain-gauge precipitation data (Katsanos *et al.* 2016, Paredes-Trejo *et al.* 2017).

2.3. Methods

To meet each objective of the study, respective methods were applied, and all the steps were performed on the Google Earth engine (GEE) platform (Gorelick *et al.* 2017). The Earth Engine is a freely available cloud-based geospatial analysis platform and hosts a multitude of remote sensing data accessible freely to users. The advantage of GEE is also the available different resources that can be utilised for the preparation of the codes for the analysis.

2.3.1 Observation of weather parameters and vegetation indices with the gaseous pollutants

For ingestion of the preparation of the S5-P OFFL products, L3 products are created in which areas within the product's bounding box containing data are searched, merged into one large mosaic creating a set of tiles containing orthorectified raster data. The procedure has been briefly summarised within the data description of each S5-P product.

The daily mean of all the weather parameters (night land surface temperature LST and day land surface temperature LST, precipitation), vegetation indices (NDVI and EVI), Sentinel-5P OFFL products (CO, HCHO, NO_2, O_3, SO_2, CH_4, Aerosol Index) was calculated at the 15-day moving average. It included averaging of the pixel values every 15 days temporally for each day, and the mean pixel value calculated from the resulting 15 day mean image regionally. LST, vegetation indices and precipitation were reprojected to the resolution of Sentinel-5P before the final regional average, and finally exported as CSV from earth engine.

Moving average is helpful in removing any outliers or extreme values, including timely data of 15 days in this case. This was continuously done from the first day to the last day of the year, annually for the years 2019, 2020, 2021 and 2022 on a separate basis. Pearson correlation was conducted to assess the relationship of all the means of all the satellite products. Applied methods have been briefly demonstrated in Figure 2.

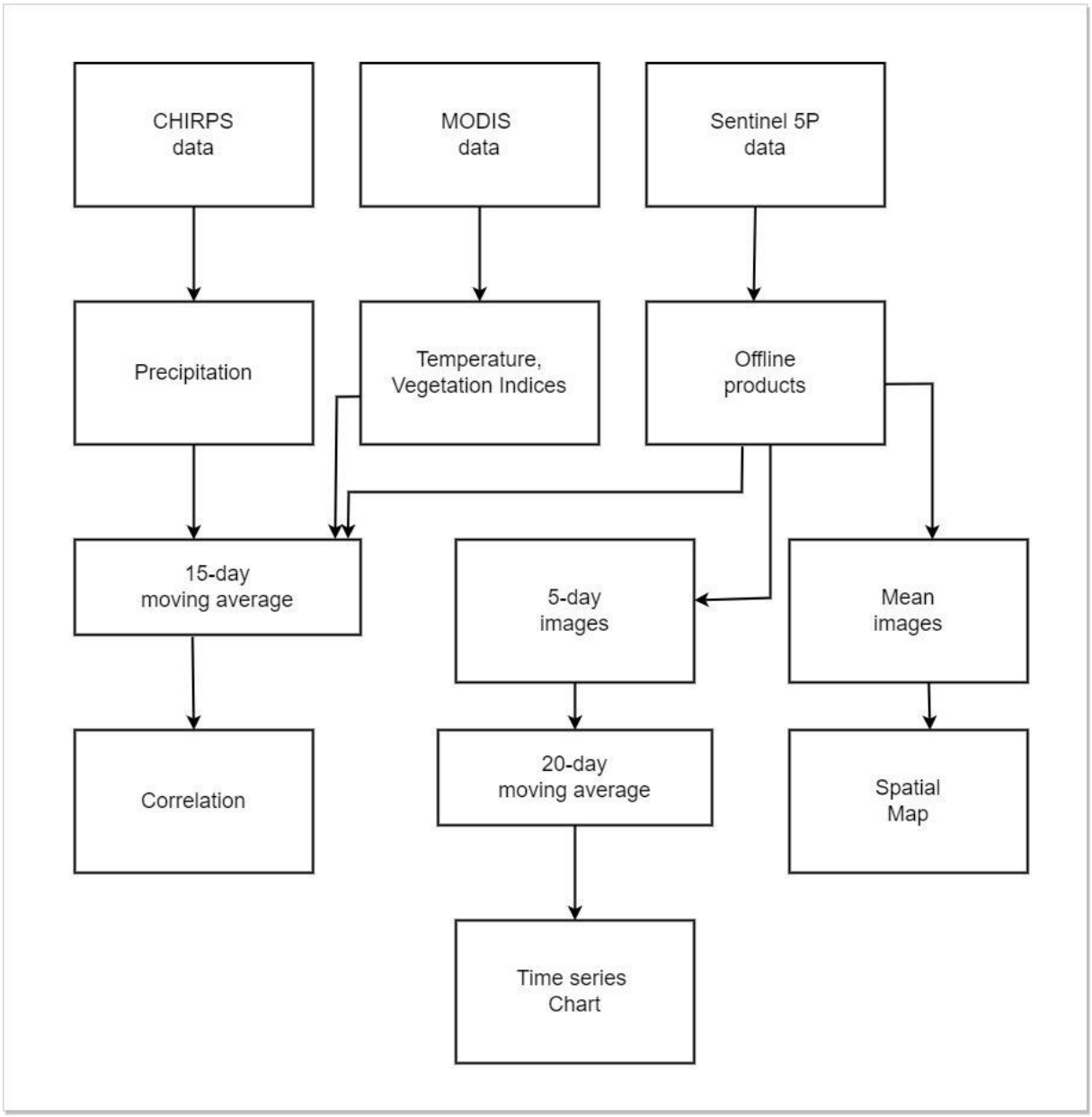

Figure 2. Flow Chart of the study

2.3.2 Yearly trends of the gaseous pollutants

The Sentinel-5P offline products were converted into 5-day images on a continuous basis from the year 2019 to 2022. This included calculating the mean image from images present within 5 days resulting in the images every 5-day interval. The mean images were made into the new image collection. Performing this reduced the time for the chart generation as charts with the daily values can result in memory error in the earth engine.

The image collection of every 5-day mean image was further smoothed with 20-day moving average. This averaged the images present within 20 days providing the new values for every 5 days smoothening the graph. The yearly values were plotted for each year with the day of the year in the X axis with values of the gaseous concentrations in different years.

2.3.3 Spatial distribution of the gaseous pollutants

Mean images to incorporate the full range of observed values, (calculated from 2019 to 2022) of the gaseous pollutants (CO, HCHO, NO_2, O_3, SO_2, CH_4) along with the aerosol index and

height over the Kathmandu district were exported from the earth engine. They were observed for the specific spatial patterns.

3. Results and Discussion

3.1 Relation of gaseous pollutants with weather parameters and vegetation indices

3.1.1 Gaseous pollutants and temperature

Temperature had highly significant negative correlations with HCHO, NO_2, SO_2 and aerosol in all the years and highly significant positive correlations with CO, O_3 and CH_4 (Tables 1). In 2019 and 2022, temperature had negative correlations with aerosol (-0.255, -0.294), NO_2 (-0.835, -0.530), SO_2 (-0.865, -0.750), HCHO (-0.079, -0.159) and positive correlations with O_3 (0.350, 0.325), CO (0.490, 0.291). Night land surface temperature showed similar correlations in both years.

Similarly, in 2020, temperature had negative correlations with aerosol (-0.267), HCHO (-0.155), NO_2 (-0.807) and positive correlation with CH_4 (0.494). In 2021, temperature had significant positive correlation with CH_4 (0.162), CO (0.458), O_3 (0.350) and negative correlation with NO_2 (-0.605). Correlations were similar for night land surface temperature in both the years 2020 and 2021.

Table 1. Pearson Correlation between gaseous pollutants with the day and night land surface temperature

	2019		*2020*		*2021*		*2022*	
	night LST	*day LST*	*night LST*	*day LST*	*night LST*	*day LST*	*night LST*	*day LST*
aer	-0.388***	-0.255***	-0.503***	-0.267***	0.042	-0.111	-0.409***	-0.294***
CH_4			0.671***	0.494***	0.450***	0.162*		
CO	0.417***	0.490***	-0.043	0.119	0.276***	0.458***	0.239***	0.291***
HCHO	-0.117*	-0.079	-0.237**	-0.155*	-0.088	0.097	-0.193***	-0.159**
NO_2	-0.850***	-0.835***	-0.770***	-0.807***	-0.684***	-0.605***	-0.622***	-0.530***
O_3	0.341***	0.350***	-0.096	0.143	0.183*	0.350***	0.203***	0.325***
SO_2	-0.859***	-0.865***	-0.708***	-0.637***	-0.580***	-0.669***	-0.698***	-0.750***

where, aer = aerosol index, CH_4 = Methane (mol fraction), CO = Carbon Monoxide (mol/m^2), HCHO= Formaldehyde (mol/m^2), NO_2 = Nitrogen Dioxide (mol/m^2), SO_2, Sulphur Dioxide (mol/m^2), LST = land surface temperature.

HCHO, SO_2. Higher temperatures can interactively participate in the chemical reaction, forming secondary pollutants and can effectively raise the heavier air above in the atmosphere in the process of convection. In heat waves, higher temperatures can increase the levels of all air pollutants, mostly increasing the ozone by more than 50 % (Kalisa *et al*. 2018). NO_2 and O_3 have been found to have a significant correlation with the temperature (Nkundabose 2020). Based on different seasonal periods, temperature has been noted with varying positive correlations with O_3, NO_2, SO_2 while NO_2 and O_3 can show negative correlations with temperature in different seasonal cases (Prabakaran *et al.* 2017). CO has also been noted to be highly correlated with temperatures (Biswas *et al.* 2020). In coastal environments SO_2 and NO_2 showed negative correlation in summer and moderately in the pre-monsoon season (Jayamurugan *et al.* 2013).

To generalise in Kathmandu, higher temperatures might have played the roles in promoting the concentrations of CH_4, CO and O_3 and suppressing the concentrations of the NO_2; This is due to the unique weather patterns or meteorological conditions within Kathmandu. Coinciding rainfall with

higher temperatures, localised wind patterns and westerly winds can contribute to the dispersion of the pollutants affecting the correlation.

3.1.2 Gaseous pollutants and precipitation

Precipitation showed a negative correlation with all the gaseous pollutants except the ozone, which in all the years showed a positive correlation of 0.352 in 2019, 0.444 in 2020, 0.404 in 2021, and 0.155 in 2022 (Table 2). Precipitation had a highly positive correlation with CO (0.329) only in 2020, and non-significant positive or negative correlations with other gaseous pollutants were seen in 2020 and 2021. But, in all cases precipitation has mostly shown negative correlations with the gaseous pollutants except the ozone.

Table 2. Pearson Correlation between gaseous pollutants with the precipitation

	precip 2019	*precip 2020*	*precip 2021*	*precip 2022*
aer	-0.260***	0.128	-0.189*	-0.748***
CH_4		-0.036	0.085	
CO	-0.021	0.329***	-0.004	-0.162**
HCHO	-0.462***	0.083	-0.059	-0.463***
NO_2	-0.524***	-0.350***	-0.148*	-0.703***
O_3	0.352***	0.444***	0.404***	0.155**
SO_2	-0.538***	-0.359***	-0.223**	-0.439***

where, aer = aerosol index, CH_4 = Methane (mol fraction), CO = Carbon Monoxide (mol/m^2), HCHO= Formaldehyde (mol/m^2), NO_2 = Nitrogen Dioxide (mol/m^2), SO_2, Sulphur Dioxide (mol/m^2), precip = precipitation (in cm followed with the year)

Precipitation has been shown to have cleaning effects on air pollutants and has the ability to completely remove the pollutants in some cases (Naresh *et al*. 2007). Concentrations of air pollutants and precipitation have always been negatively correlated (Liu *et al*. 2020, Maboa *et al*. 2022). Precipitations usually improve the air quality in the process; however, in rare cases, reduction of vertical convection in the atmosphere can sometimes have negative effects on the air quality (Tian *et al*. 2021). This or due to the other reasons the CO concentrations should have been positively correlated in the year 2020. For ozone, the precipitation might have caused the downward shifts and thus resulting higher concentrations of the ozone.

3.1.3 Gaseous pollutants with vegetation indices

The correlation of both the EVI and NDVI showed varied relations with the gaseous pollutants (Table 3). In 2019 and 2022, respectively, the correlations of EVI with NO_2 were -0.431 and -0.028, SO_2 were -0.400 and 0.006, O_3 were 0.099 and -0.397, CO were 0.102 and -0.453, HCHO 0.025 and -0.012. Negative correlations were seen both in 2020 and 2021 in CO (-0.177, -0.629), HCHO (-0.270, -0.529), NO_2 (-0.547, -0.205), O_3 (-0.460, -0.569), and positive correlations with CH_4 (0.865, 0.681).

With EVI, Aerosol had a positive correlation in the year 2021 (0.451) and a non-significant positive correlation in 2022 (0.033), whereas negative in 2019 (0.680) and 2020 (-0.619). In 2019 and 2022, NDVI had negative correlation with ozone (-0.143, -0.400). Although non-significant negative correlation of NDVI and aerosol -0.073 is seen in 2019, highly significant positive correlation was seen in 2022. This was visible in 2020 and 2021 with -0.477 and 0.399 respectively.

Likewise, the significant non-negative correlation between CO and NDVI is seen in 2022, whereas a positive correlation of 0.161 is seen in 2019. NDVI showed highly significant positive

correlation with HCHO (0.502 in 2019, 0.453 in 2022), NO_2 (0.336 in 2019, 0.691 in 2022), SO_2 (0.351 in 2019, 0.429 in 2022). However, in 2020 and 2021, the correlations of NDVI with CO (-0.232, -0.468), HCHO (-0.164, -0.233), O_3 (-0.501, -0.508) and NO_2 (-0.319, -0.023) were negative. CH_4 had a highly significant positive correlation with NDVI in both 2020 and 2021, with 0.695 and 0.250, respectively.

Table 3. Pearson Correlation between gaseous pollutants with the vegetation indices

	2019		*2020*		*2021*		*2022*	
	EVI	*NDVI*	*EVI*	*NDVI*	*EVI*	*NDVI*	*EVI*	*NDVI*
aer	-0.619***	-0.073	-0.680***	-0.477***	0.451***	0.399***	0.033	0.748***
CH_4			0.865***	0.695***	0.681***	0.250***		
CO	0.102	0.161**	-0.177*	-0.232**	-0.629***	-0.468***	-0.453***	-0.126*
HCHO	0.025	0.502***	-0.270***	-0.164*	-0.529***	-0.233**	-0.122*	0.453***
NO_2	-0.431***	0.336***	-0.547***	-0.319***	-0.205**	-0.023	-0.028	0.691***
O_3	0.099	-0.143**	-0.460***	-0.501***	-0.569***	-0.508***	-0.397***	-0.400***
SO_2	-0.400***	0.351***	-0.452***	-0.128	0.324***	0.414***	0.006	0.429***

where, aer = aerosol index, CH_4 = Methane (mol fraction), CO = Carbon Monoxide (mol/m^2), HCHO= Formaldehyde (mol/m^2), NO_2 = Nitrogen Dioxide (mol/m^2), SO_2, Sulphur Dioxide (mol/m^2), EVI = Enhanced Vegetation Index, NDVI = Normalised Difference Vegetation Index

NDVI and EVI are usually associated with the level of greenness due to the presence of vegetation. Vegetation playing roles in the controlling of air pollutants has been shown to be in limited quantity, and this is more evident when the growing season is short for the vegetation (Setälä *et al*. 2013). The type of vegetation, the denseness, the tallness and the closeness of the vegetation have been found to be responsible for how the air pollutants are impacted (Janhäll 2015). However, the direct and indirect impacts of the vegetation are evident as the vegetation can lower the air temperature, change the direction of the wind and block the solar radiation, inhibiting or slowing any temperature-dependent reaction of air pollutants (Nowak *et al*. 1998). Oppositely, air pollutants can be toxic and detrimental for the health of the vegetation (Emberson *et al*. 2001).

EVI is seen as more robust, showing negative correlations even when the NDVI is seen showing positive correlations with the air pollutants. The robustness of EVI has been noted with its ability to detect dense vegetation areas and canopy structures(Huete *et al.* 2002). Despite vegetation indices having shown the negative correlation with the air pollutants, conclusively, it still cannot be said that the vegetation meaningfully reduced the air pollutants as vegetation can be the result of the changing seasons. It can be inferred, however, that vegetation may play a significant role in mitigating the gaseous pollutants.

3.1.4 Gaseous pollutants with gaseous pollutants

Tables 4 and 5 show the diverse correlation between gaseous pollution over the years. Aerosol had positive correlation with all of the other pollutants except ozone. Negative correlations were seen in 2019 (-0.109), 2021 (-0.058), 2022 (-0.154) and positive in 2020 (-0.596). With CH_4, aerosol had contradicting correlations of 0.485 in 2021, and -0.768 in 2020. CH_4 showed a negative correlation with most of the gaseous pollutants, which was visible in both 2020 and 2021.

Table 4: Pearson Correlation between gaseous pollutants (lower triangle: 2020, upper triangle: 2021)

	aer	*CH_4*	*CO*	*HCHO*	*NO_2*	*O_3*	*SO_2*
aer		0.485***	0.091	0.303***	0.191*	-0.058	0.472***
CH_4	-0.768***		-0.118	-0.298***	-0.438***	-0.333***	-0.099
CO	0.478***	-0.142		0.700***	-0.042	0.362***	-0.542***
HCHO	0.450***	-0.148*	0.458***		0.398***	0.496***	0.063
NO_2	0.191*	-0.252***	0.032	0.450***		0.051	0.591***
O_3	0.596***	-0.665***	0.366***	-0.136	-0.330***		-0.09****
SO_2	0.340***	-0.255***	0.094	0.443***	0.658***	-0.260***	

where, aer = aerosol index, CH_4 = Methane (mol fraction), CO = Carbon Monoxide (mol/m^2), HCHO= Formaldehyde (mol/m^2), NO_2 = Nitrogen Dioxide (mol/m^2), SO_2, Sulphur Dioxide (mol/m^2)

CO had a positive correlation with all the gaseous pollutants, except with SO_2, which showed negative correlations of -0.238 in 2019, -0.542 in 2021, -0.235 in 2022, and a non-significant positive correlation of 0.094 in 2020. CO similarly showed non-significant positive correlations in 2020 and 2021. SO_2 mostly showed negative correlations with CO and O_3 which is visible in all the years.

HCHO showed positive correlations with all of the other pollutants except negative correlation -0.148 with CH_4 and non-significant negative correlation of -0.07 with O_3 in 2022.

NO_2 had negative correlations of -0.188 with CO and -0.275 O_3 in 2019. The correlation with O_3 and NO_2 in 2020 was -0.330, 2022 was -0.300, and non-significant positive correlation of 0.051 in 2021. It showed a positive correlation of 0.153 with CO in 2022.

Table 5: Pearson Correlation between gaseous pollutants (lower triangle: 2019, upper triangle 2022)

	aer	*CO*	*HCHO*	*NO_2*	*O_3*	*SO_2*
aer		0.234***	0.691***	0.801***	-0.154**	0.353***
CO	0.376***		0.509***	0.153**	0.480***	-0.235***
HCHO	0.413***	0.557***		0.622***	-0.07	0.306***
NO_2	0.457***	-0.188***	0.381***		-0.300***	0.509***
O_3	-0.109*	0.281***	0.089	-0.275***		-0.540***
SO_2	0.253***	-0.238***	0.290***	0.755***	-0.141**	

where, aer = aerosol index, CO = Carbon Monoxide (mol/m^2), HCHO= Formaldehyde (mol/m^2), NO_2 = Nitrogen Dioxide (mol/m^2), SO_2, Sulphur Dioxide (mol/m^2)

The negative correlations of the gaseous pollutants can be explained by their chemical reactivities while the positive correlation can be due to the same source of the gaseous pollutants. For instance, reactions of NO_2 and O_3 are explainable by the equilibrium reaction of NO_2 forming O_3, and vice versa. These gases can effectively reduce each other's concentrations. Similarly, gases such as CH_4 and NO_2 can trap the heat causing the greenhouse effect influencing the presence of other gases.

3.2 Yearly trends of the gaseous pollutants.

Yearly observations of the trends or evolutions of the gaseous pollutants revealed distinct patterns in the concentrations of the air pollutants throughout the year. Lower concentrations of the gaseous pollutants in the year 2020 could be interpreted towards the effects of the COVID-19 outbreak. The Aerosol Index was lowest in the year 2020, which is lowest compared to other years, and the index is seen highest in 2022 (Figure 3).

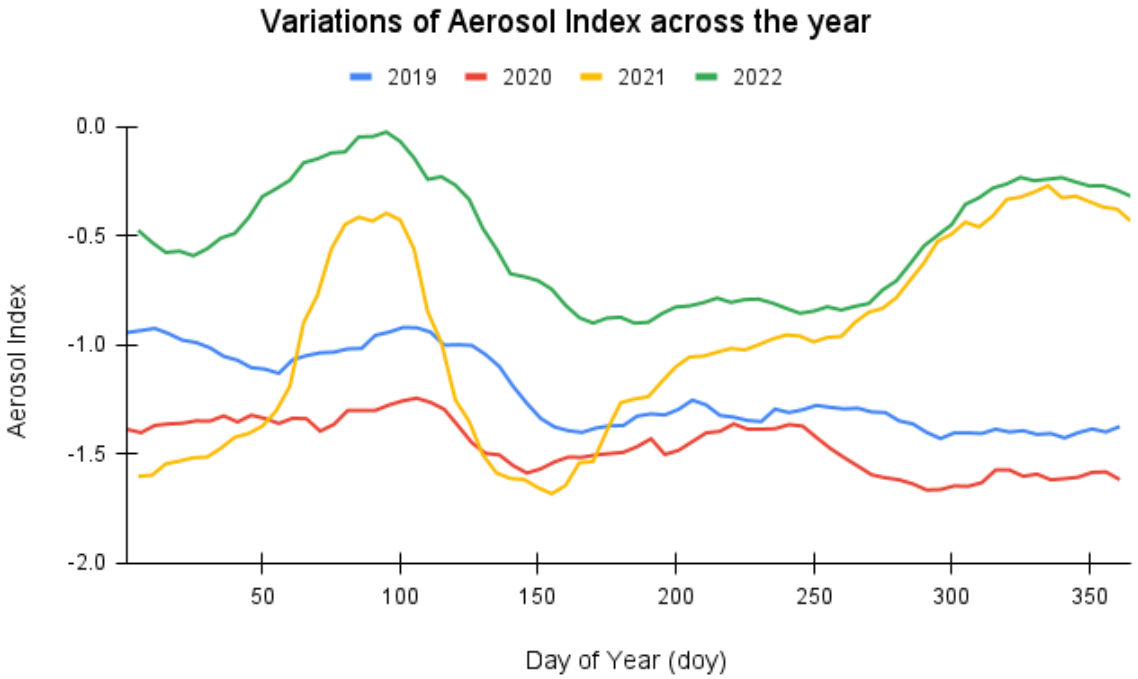

Figure 3. Aerosol Index in different days of the years (2019-2022)

In SO_2 (Figure 4), the pollutants seemed to be in higher concentrations in initial months compared to the mid months of the year which eventually increased at the end of the year which is seen in similar trends in all the four years from 2019 to 2022. Similarity is seen in the O_3 with the concentrations becoming massive in the initial months which subsidies in the later part of the months with minor increasing at the end of the months (Figure 5). Higher concentrations of O_3 in the early months of April, May and June has also been confirmed by Kondo *et al*. (2005) as the solar radiation is strong in those months. Between 150 to 300 days of the month in the year 2020, concentrations of O_3 is comparatively lower in comparison to other years indicative of the COVID-19 reducing in the concentrations although the concentrations were similarly higher in the beginning of the year.

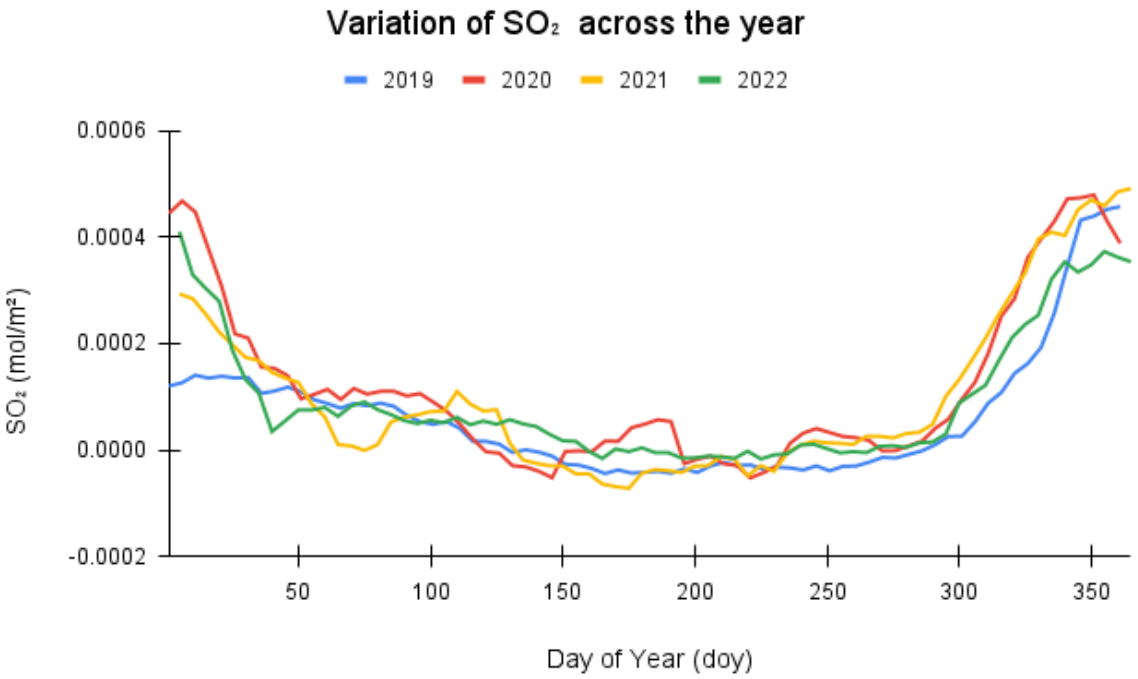

Figure. 4. SO_2 concentrations in different days of the years (2019-2022)

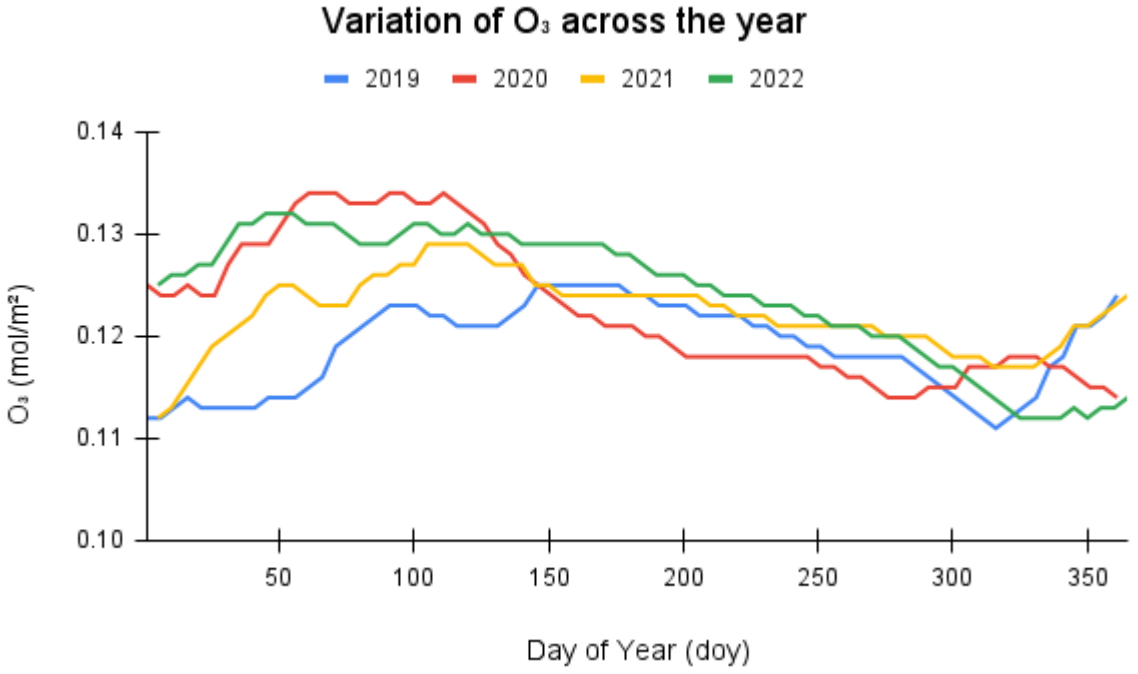

Figure 5. O3 concentrations in different days of the years (2019-2022)

The same logic can be applied to the NO_2 concentrations where the concentrations are seen lowest in 2020 if compared among four years and the concentrations are seen getting higher in 2021 and 2022 (Figure 6). NO_2 concentrations seemed to increase towards the end of year. Relatable trends are visible in concentrations of HCHO as the concentrations are lower in 2020 when compared to other years (Figure 7).

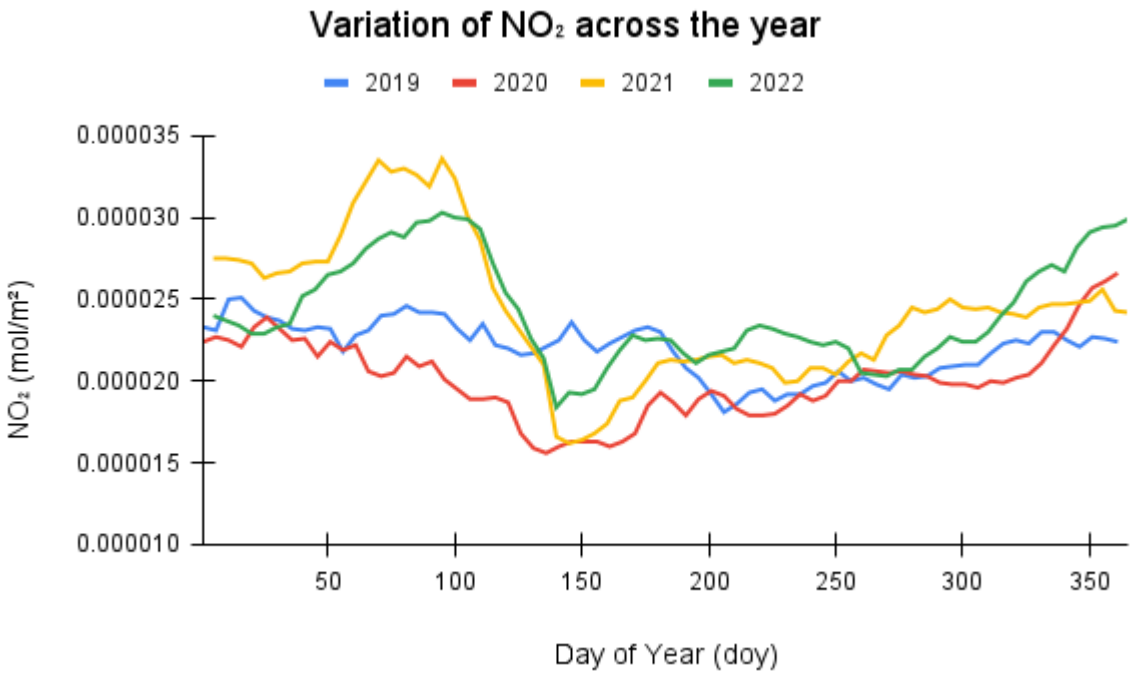

Figure 6. NO_2 concentrations in different days of the years (2019-2022)

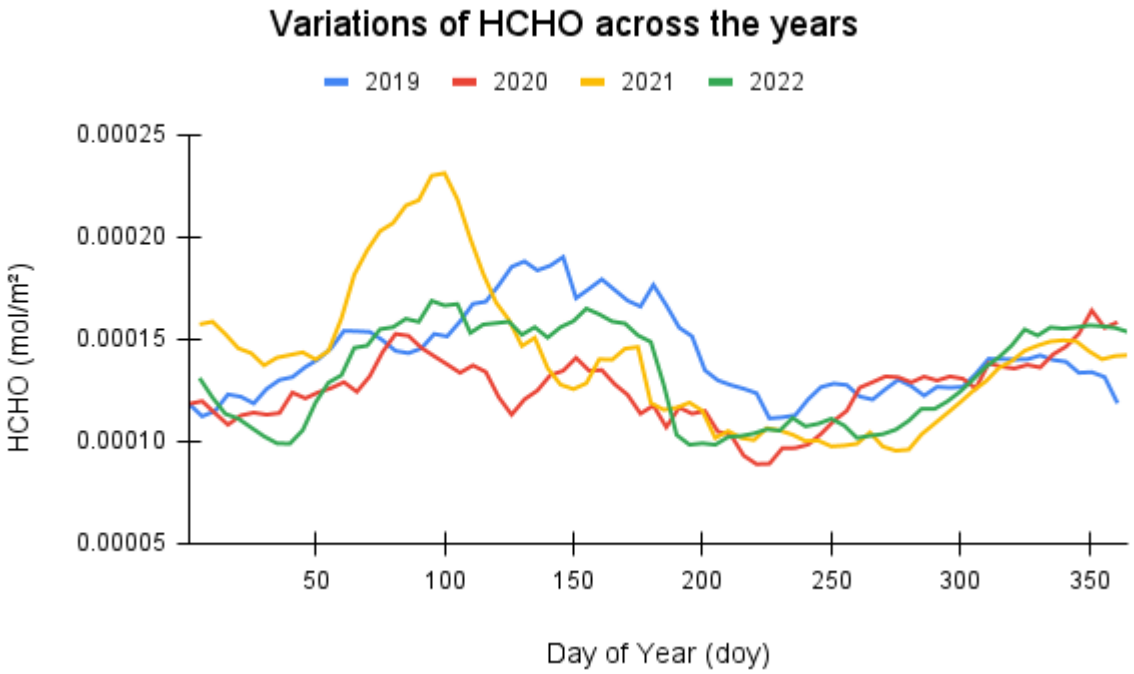

Figure 7. HCHO concentrations in different days of the years (2019-2022)

For the concentrations of CO and CH_4, the concentration changes cannot be interpretatively assigned to COVID-19 as the concentration of the year 2020 are not indistinguishable with the other years; CO concentrations seem to be higher in initial months of 2021 compared to other years (Figure 8). CH_4 concentrations were lowest in 2019 and the concentrations were higher in other years (Figure 9). Missing data in the months has resulted in the discontinuous chart.

Higher concentrations of air pollutants such as CO, NO_2, HCHO, and aerosol in 2021 can be assumed towards the forest fire happening within or in the nearby districts which pollutes the

atmosphere of Kathmandu district (Aljazeera 2021). Forest fires are usually seen from January to June in Nepal with major occurrences seen in April (Bhujel *et al.* 2022). These occurrences are common in neighbouring districts or within Kathmandu which severely impacts the air within the district.

Decrease of air pollutants during the COVID-19 lockdown has been noted in multiple works which is logical to assume in the decreased concentrations of gaseous pollutants in 2020 (Ali *et al*. 2021, Dhital *et al*. 2022, Majumder *et al*. 2021).

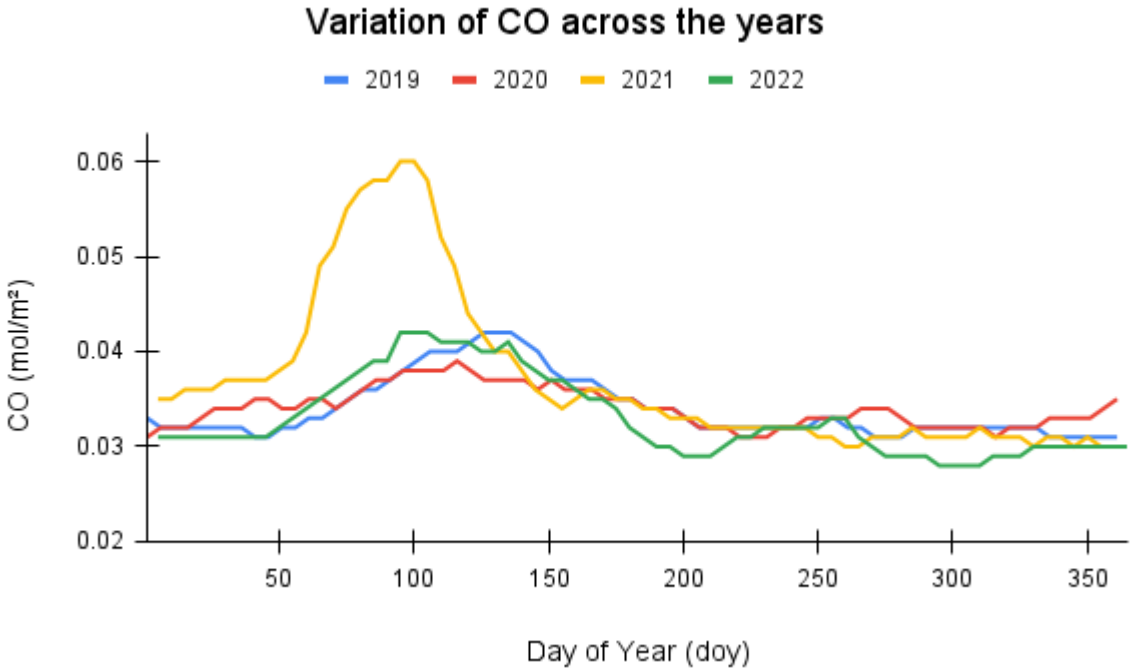

Figure 8. CO concentrations in different days of the years (2019-2022)

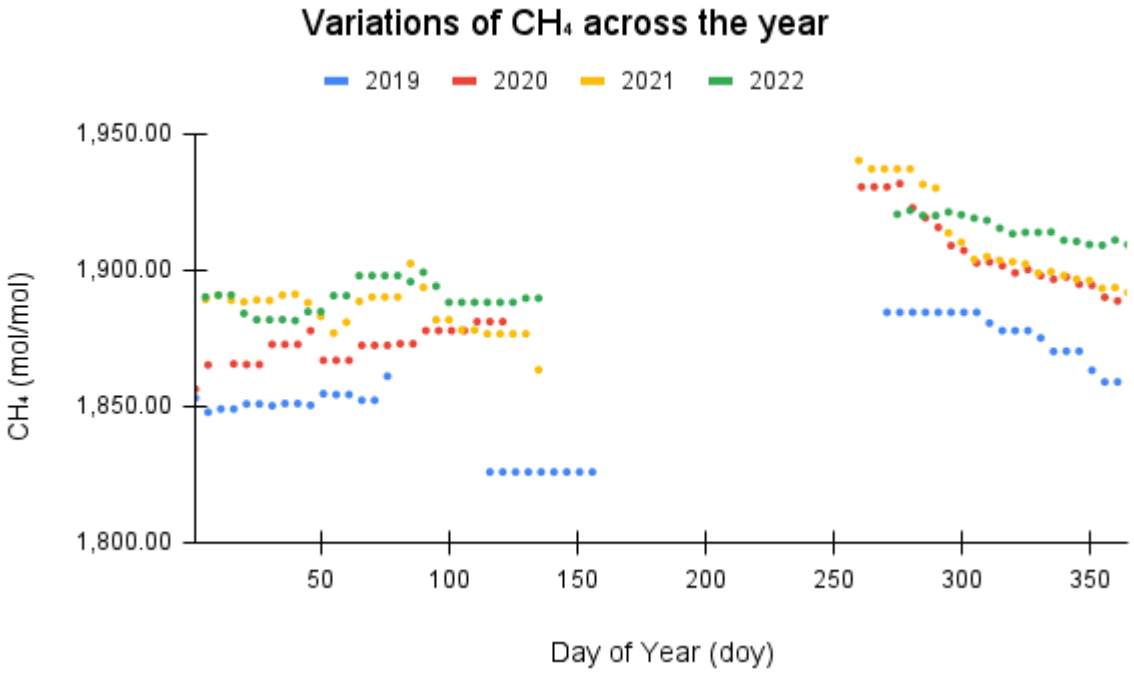

Figure 9. CH_4 concentrations on different days of the year (2019-2022)

3.3 Spatial Distribution of the gaseous pollutants

Spatial patterns of the gaseous pollutants were distinct in their spatial distribution (Figure 10). NO_2 seemed to be located particularly at the centre of the district, distinctive compared to other gaseous pollutants. CO, HCHO and O_3 were mostly located at the centre of the district but distributed around the boundaries of the district. SO_2 and CH_4 had different spatial distributions compared to other gaseous pollutants as they were not particularly concentrated within the district. CH_4 showed some spatial locations where its locations were higher or lower compared to other areas and it was evenly distributed around the areas of the district. SO_2 had no distinctive patterns of its concentration and higher concentrations were rather distributed within the district. These spatial patterns provide insights into their geo-location while explaining their sources, further suggesting their pathways.

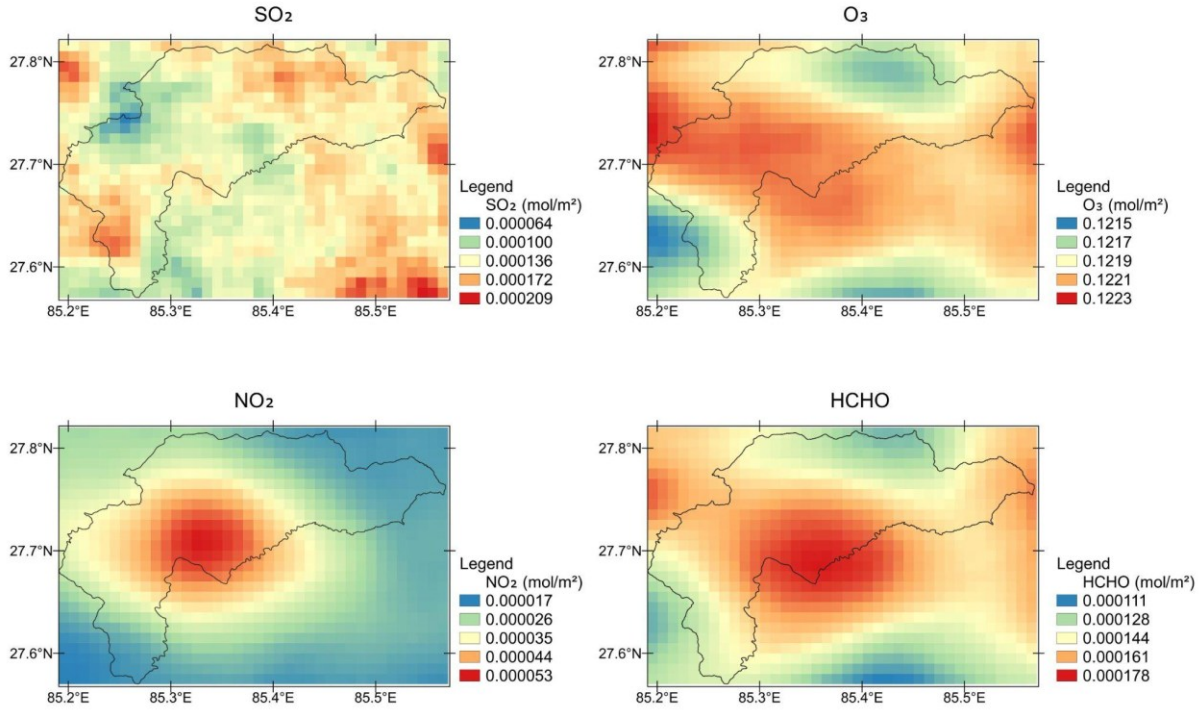

Figure 10. Spatial Distribution of different gaseous pollutants in Kathmandu District (Averaged 2019-2022)

The Aerosol index is seen lower in the central parts of the district comparatively (Figure 11). As this is the mean image, the value ranges from -1.26 to -0.79, implying a lower presence of aerosols in the atmosphere. This can certainly vary with locations and time. Aerosol height had the highest mean height in the mid part of the district while some areas near the northern and southern boundaries with lower aerosol height. These can be explained by the topography and the local winds playing the role in their movement as aerosol moves out of the valley through the wind corridor (Pokhrel *et al.* 2021).

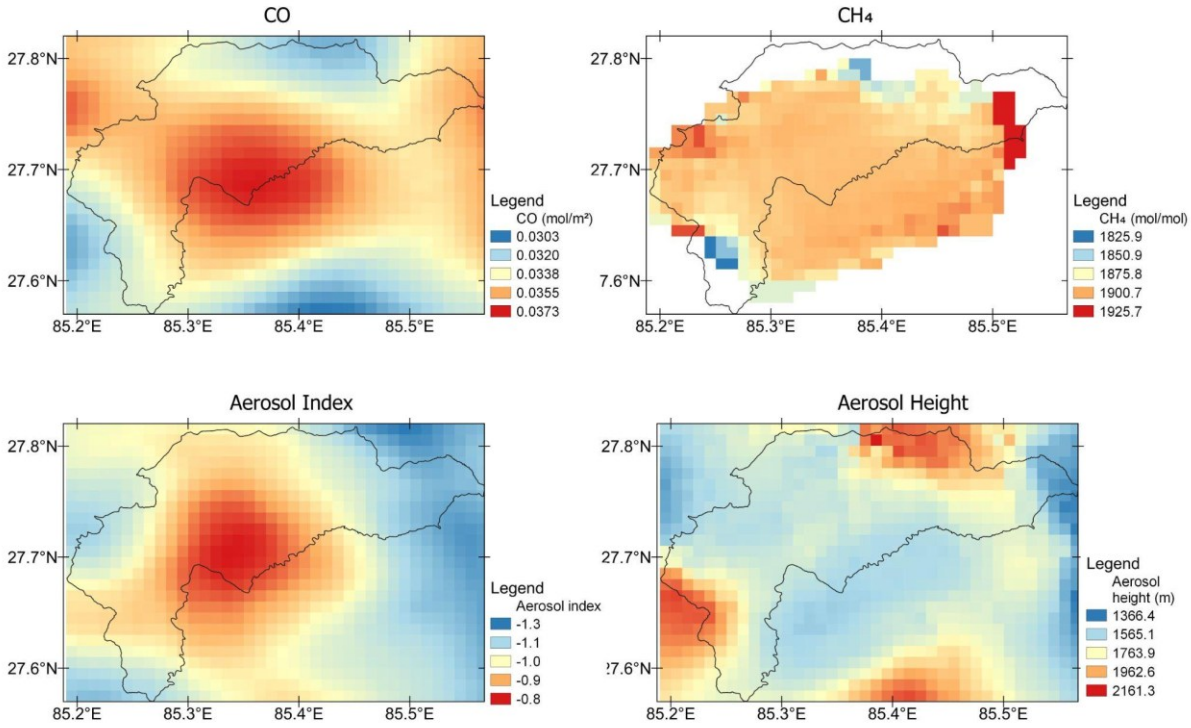

Figure 11. Spatial Distribution of CO, CH_4, aerosol index and aerosol height (Averaged 2019-2022)

3.4 Interpretations of the results

As per the objectives, different methods were applied, and the relation of the concentrations of the pollutants with different dynamics was expressively observed.

Firstly, the significant or non-significant correlations between weather parameters (temperature and precipitation) with the gaseous pollutants have hinted at the direct or indirect impacts ofthe change of the air pollutants. What can be conclusively stated is the precipitation should have always reduced the air pollutants in the atmosphere except the ozone. Temperature plays different reducing roles depending on the gaseous pollutants. Vegetation, represented by Enhanced Vegetation Index (EVI) was seen having negative correlation with most of the gaseous pollutants which may point in the roles of the vegetation in controlling the air pollution directly or indirectly. Secondly, the trends of the air pollutants over the days of the year have shown the effects of COVID-19 on some of the air pollutants, as the concentrations were lesser in 2020 compared to the other years. This could be confirmed by the lowest aerosol index in the year 2020. This was, however, not always true for all the gaseous pollutants.

Thirdly, the spatial distribution was unique for all the gaseous pollutants. NO_2 for instance is mostly concentrated at the district's centre and other gaseous pollutants are distributed around the district. This could be clearly understood as the capital of Nepal, Kathmandu, is the most urbanised city where most of the pollutants are being generated.

Limitations of the study can still be pointed out. The concentrations from the satellite, Sentinel-5P in this case, still cannot be directly interpreted as the pollutants in the ground. And, the homogeneity of the air pollutants can never be confirmed which is in continuous change. Influence from the other factors such as wind, seasons or atmospheric pressure have not been explored. The inclusion of higher temporal resolution has however allowed the observation of the yearly trends. The other limitations are in how to consider what levels of the concentrations of the air pollutants retrieved from the satellite be considered as the thresholds above which might be detrimental to human health.

Future works can relate the Sentinel-5P data with the ground-based air sensor data of Kathmandu and nearby districts that can be assessed with regression methods.

The advantages of using satellite data in the inspection of air pollutants have been made visible in this paper. For observing the concentrations of the air pollutants, the satellite data Sentinel-5P, in larger spatial dimensions will boldly be scientific.

4. Conclusions

In this researchS5-P data was used to correlate with the weather parameters (temperature and precipitation) and vegetation indices to understand the impact of the external factors in the gaseous pollutants. It can be concluded that the temperature and vegetation can play an essential role in minimising the activities of the gaseous pollutants. Precipitation can directly attenuate the presence of almost all the gaseous pollutants except the ozone.

It is also visible how the COVID-19 lockdown impacted the decrease of the concentrations of the gaseous pollutants. The spatial distribution of the gaseous pollutants, which are uniquely present in the Kathmandu district, is also visible.

Overall, the scientific importance of S5-P in studying gaseous pollutants can be highlighted. Proper vegetation within the city and balancing the city's temperature are likely to ease the gaseous pollutants.

6. Acknowledgments

The author sincerely appreciates the reviewers and the editors for assisting with the refinement of this work. The author also acknowledges the journal for allowing the article to be published.

References

AbdelSattar, D. A. (2019). Monitoring Air Pollution Using Satellite Data. *Saudi Arabia*.

Ali, G., Abbas, S., Qamer, F. M., Wong, M. S., Rasul, G., Irteza, S. M., Shahzad, N. (2021). Environmental impacts of shifts in energy, emissions, and urban heat island during the COVID-19 lockdown across Pakistan. *Journal of Cleaner Production*, *291*, 125806. https://doi.org/10.1016/j.jclepro.2021.125806

Aljazeera. (2021). *Nepal battles worst forest fires in years as air quality drops*. https://www.aljazeera.com/news/2021/4/9/nepal-battles-worst-forest-fires-in-years-as-air-quality-drops

Bernstein, J. A., Alexis, N., Barnes, C., Bernstein, I. L., Nel, A., Peden, D., Diaz-Sanchez, D., Tarlo, S. M., Williams, P. B., Bernstein, J. A. (2004). Health effects of air pollution. *Journal of Allergy and Clinical Immunology*, *114*(5), 1116–1123. https://doi.org/10.1016/j.jaci.2004.08.030

Bhujel, K. B., Sapkota, R. P., Khadka, U. R. (2022). Temporal and Spatial Distribution of Forest Fires and their Environmental and Socio-economic Implications in Nepal. *Journal of Forest and Livelihood*, *21*(1), 1–13. https://doi.org/10.3126/jfl.v21i1.56575

Biswas, K., Chatterjee, A., Chakraborty, J. (2020). Comparison of Air Pollutants Between Kolkata and Siliguri, India, and Its Relationship to Temperature Change. *Journal of Geovisualization and Spatial Analysis*, 4(2), 25. https://doi.org/10.1007/s41651-020-00065-4

Bodah, B. W., Neckel, A., Stolfo Maculan, L., Milanes, C. B., Korcelski, C., Ramírez, O., Mendez-Espinosa, J. F., Bodah, E. T., Oliveira, M. L. S. (2022). Sentinel-5P TROPOMI satellite application for NO_2 and CO studies aiming at environmental valuation. *Journal of Cleaner Production*, *357*, 131960. https://doi.org/10.1016/j.jclepro.2022.131960

Dhital, N. B., Bhattarai, D. R., Sapkota, R. P., Rijal, K., Byanju, R. M., Yang, H.-H. (2022). Comparing the Change in Air Quality during the COVID-19 Lockdown between Dry and Wet Seasons

in Nepal. *Aerosol and Air Quality Research*, 22. https://doi.org/10.4209/aaqr.220201.

Emberson, L. D., Ashmore, M. R., Murray, F., Kuylenstierna, J. C. I., Percy, K. E., Izuta, T., Zheng, Y., Shimizu, H., Sheu, B. H., Liu, C. P., Agrawal, M., Wahid, A., Abdel-Latif, N. M., van Tienhoven, M., de Bauer, L. I., Domingos, M. (2001). Impacts of Air Pollutants on Vegetation in Developing Countries. *Water, Air, and Soil Pollution*, 130(1), 107–118. https://doi.org/10.1023/A:1012251503358.

ESA. (n.d.-a). *Sentinel-5P*. https://www.esa.int/Applications/Observing_the_Earth/Copernicus/Sentinel-5P.

ESA. (n.d.b). *Facts and figures*. https://www.esa.int/Applications/Observing_the_Earth/Copernicus/Sentinel-5P/Facts_and_figures.

Fuertes, E., van der Plaat, D. A., Minelli, C. (2020). Antioxidant genes and susceptibility to air pollution for respiratory and cardiovascular health. *Free Radical Biology and Medicine*, 151, 88–98. https://doi.org/10.1016/j.freeradbiomed.2020.01.181.

Fuller, R., Landrigan, P. J., Balakrishnan, K., Bathan, G., Bose-O'Reilly, S., Brauer, M., Caravanos, J., Chiles, T., Cohen, A., Corra, L., Cropper, M., Ferraro, G., Hanna, J., Hanrahan, D., Hu, H., Hunter, D., Janata, G., Kupka, R., Lanphear, B., … Yan, C. (2022). Pollution and health: A progress update. *The Lancet Planetary Health*, 6(6), e535–e547. https://doi.org/10.1016/S2542-5196(22)00090-0.

Funk, C., Peterson, P., Landsfeld, M., Pedreros, D., Verdin, J., Shukla, S., Husak, G., Rowland, J., Harrison, L., Hoell, A., Michaelsen, J. (2015). The climate hazards infrared precipitation with stations—A new environmental record for monitoring extremes. *Scientific Data*, 2. https://doi.org/10.1038/sdata.2015.66

Gao, K. & Yuan, Y. (2022). Is the sky of smart city bluer? Evidence from satellite monitoring data. *Journal of Environmental Management*, *317*, 115483. https://doi.org/10.1016/j.jenvman.2022.115483

Glencross, D. A., Ho, T.-R., Camiña, N., Hawrylowicz, C. M., Pfeffer, P. E. (2020). Air pollution and its effects on the immune system. *Free Radical Biology and Medicine*, 151, 56–68. https://doi.org/10.1016/j.freeradbiomed.2020.01.179.

Gorelick, N., Hancher, M., Dixon, M., Ilyushchenko, S., Thau, D., Moore, R. (2017). Google Earth Engine: Planetary-scale geospatial analysis for everyone. *Remote Sensing of Environment*, 202, 18–27 https://doi.org/10.1016/j.rse.2017.06.031.

Gulia, S., Shiva Nagendra, S. M., Khare, M., Khanna, I. (2015). Urban air quality management-A review. *Atmospheric Pollution Research*, 6(2), 286–304. https://doi.org/10.5094/APR.2015.033.

Holloway, T., Miller, D., Anenberg, S., Diao, M., Duncan, B., Fiore, A. M., Henze, D. K., Hess, J., Kinney, P. L., Liu, Y., Neu, J. L., O'Neill, S. M., Odman, M. T., Pierce, R. B., Russell, A. G., Tong, D., West, J. J., Zondlo, M. A. (2021). Satellite Monitoring for Air Quality and Health. *Annual Review of Biomedical Data Science*, *4*, 417–447. https://doi.org/10.1146/annurev-biodatasci-110920-093120

Huete, A., Didan, K., Miura, T., Rodriguez, E. P., Gao, X., Ferreira, L. G. (2002). Overview of the radiometric and biophysical performance of the MODIS vegetation indices. *Remote Sensing of Environment*, *83*(1), 195–213.. https://doi.org/10.1016/S0034-4257(02)00096-2

Huete, A., Didan, K., van Leeuwen, W., Miura, T., Glenn, E. (2011). MODIS Vegetation Indices. In B. Ramachandran, C. O. Justice, M. J. Abrams (Eds.), *Land Remote Sensing and Global Environmental Change: NASA's Earth Observing System and the Science of ASTER and MODIS*. (579–602). Springer. https://doi.org/10.1007/978-1-4419-6749-7_26.

Janhäll, S. (2015). Review on urban vegetation and particle air pollution – Deposition and dispersion. *Atmospheric Environment*, 105, 130–137. https://doi.org/10.1016/j.atmosenv.2015.01.052

Jayamurugan, R., Kumaravel, B., Palanivelraja, S., Chockalingam, M. P. (2013). Influence of Temperature, Relative Humidity and Seasonal Variability on Ambient Air Quality in a Coastal Urban Area. *International Journal of Atmospheric Sciences*, 2013, e264046. https://doi.org/10.1155/2013/264046

Kalisa, E., Fadlallah, S., Amani, M., Nahayo, L., Habiyaremye, G. (2018). Temperature and air pollution relationship during heatwaves in Birmingham, UK. *Sustainable Cities and Society*, 43, 111–120. https://doi.org/10.1016/j.scs.2018.08.033

Kampa, M. & Castanas, E. (2008). Human health effects of air pollution. *Environmental Pollution*, 151(2), 362–367. https://doi.org/10.1016/j.envpol.2007.06.012

Kaplan, G. & Avdan, Z. Y. (2020). Space-borne air pollution observation from Sentinel-5p Tropomi: Relationship between pollutants, geographical and demographic data. *International Journal of Engineering and Geosciences*, 5(3). https://doi.org/10.26833/ijeg.644089

Kaplan, G., Avdan, Z. Y., Avdan, U. (2019). Spaceborne Nitrogen Dioxide Observations from the Sentinel-5P TROPOMI over Turkey. *Proceedings*, 18(1). https://doi.org/10.3390/ECRS-3-06181

Karki, R., Talchabhadel, R., Aalto, J., Baidya, S. K. (2016). New climatic classification of Nepal. *Theoretical and Applied Climatology,* 125(3–4), 799–814. https://doi.org/10.1007/s00704-015-1549-0

Katsanos, D., Retalis, A., Michaelides, S. (2016). Validation of a high-resolution precipitation database (CHIRPS) over Cyprus for a 30-year period. *Atmospheric Research*, 169, 459–464. https://doi.org/10.1016/j.atmosres.2015.05.015

Kondo, A., Kaga, A., Imamura, K., Inoue, Y., Sugisawa, M., Shrestha, M. L., Sapkota, B. (2005). Investigation of air pollution concentration in Kathmandu valley during winter season. *Journal of Environmental Sciences (China)*, 17(6), 1008–1013.

Liu, Y., Zhou, Y., Lu, J. (2020). Exploring the relationship between air pollution and meteorological conditions in China under environmental governance. *Scientific Reports*, 10(1), Article 1. https://doi.org/10.1038/s41598-020-71338-7

Maboa, R., Yessoufou, K., Tesfamichael, S., Shiferaw, Y. A. (2022). Sizes of atmospheric particulate matters determine the outcomes of their interactions with rainfall processes. *Scientific Reports*, 12. https://doi.org/10.1038/s41598-022-22558-6

Magro, C., Nunes, L., Gonçalves, O. C., Neng, N. R., Nogueira, J. M. F., Rego, F. C., Vieira, P. (2021). Atmospheric Trends of CO and CH_4 from Extreme Wildfires in Portugal Using Sentinel-5P TROPOMI Level-2 Data. *Fire*, 4(2), Article 2. https://doi.org/10.3390/fire4020025

Majumder, A. K., Nayeem, A. A., Islam, M., Carter, W. S., Razib, Khan, S. M. H. (2021). Effect of COVID-19 Lockdown on Air Quality: Evidence from South Asian Megacities: 10.32526/ennrj/19/2020230. *Environment and Natural Resources Journal*, 19(3), Article 3.

Naresh, R., Sundar, S., Shukla, J. B. (2007). Modeling the removal of gaseous pollutants and particulate matters from the atmosphere of a city. *Nonlinear Analysis: Real World Applications*, 8(1), 337–344. https://doi.org/10.1016/j.nonrwa.2005.08.005

Nkundabose, J. P. (2020). *Establishing Relationship between Meteorological Parameters and Criteria Air Pollutants Concentration in Delhi* (SSRN Scholarly Paper 3800806). https://papers.ssrn.com/abstract=3800806

Nowak, D. J., McHale, P. J., Ibarra, M., Crane, D., Stevens, J. C., Luley, C. J. (1998). Modeling the Effects of Urban Vegetation on Air Pollution. In S.-E. Gryning & N. Chaumerliac (Eds.), *Air Pollution Modeling and Its Application XII* (pp. 399–407). Springer US. https://doi.org/10.1007/978-1-4757-9128-0_41

Paredes-Trejo, F. J., Barbosa, H. A., Lakshmi Kumar, T. V. (2017). Validating CHIRPS-based satellite precipitation estimates in Northeast Brazil. *Journal of Arid Environments,* 139, 26–40. https://doi.org/10.1016/j.jaridenv.2016.12.009

Phan, T. N., Kappas, M. (2018). Application of MODIS land surface temperature data: A systematic literature review and analysis. *Journal of Applied Remote Sensing*, *12*(4), 041501. https://doi.org/10.1117/1.JRS.12.041501

Pokhrel, R., Lee, H., Sharma, R. K., & Sapkota, B. (2021). Aerosol Dispersion Over a High Altitude

Region: A Case Study of Kathmandu, Nepal. *Water, Air, & Soil Pollution*, *232*. https://doi.org/10.1007/s11270-021-05007-4

Prabakaran, P., Krishnasamy, V., Ayyar, M., Rambabu, V. (2017). Consequence of Meteorological Factors on Gaseous Pollutants and Seasonal Erraticism in the Ambient Air of Chennai City. *Indian Journal of Environmental Protection*, *37*, 461–474.

Ritchie, H. & Roser, M. (2019). Outdoor Air Pollution. *Our World in Data*. https://ourworldindata.org/outdoor-air-pollution

Saud, B. & Paudel, G. (2018). The Threat of Ambient Air Pollution in Kathmandu, Nepal. *Journal of Environmental and Public Health*, *2018*, e1504591. https://doi.org/10.1155/2018/1504591

Schneider, P., Hamer, P. D., Kylling, A., Shetty, S., Stebel, K. (2021). Spatiotemporal Patterns in Data Availability of the Sentinel-5P NO_2 Product over Urban Areas in Norway. *Remote Sensing*, *13*(11), Article 11. https://doi.org/10.3390/rs13112095

Setälä, H., Viippola, V., Rantalainen, A.-L., Pennanen, A., Yli-Pelkonen, V. (2013). Does urban vegetation mitigate air pollution in northern conditions? *Environmental Pollution*, *183*, 104–112. https://doi.org/10.1016/j.envpol.2012.11.010

Sicard, P., Agathokleous, E., Anenberg, S. C., De Marco, A., Paoletti, E., Calatayud, V. (2023). Trends in urban air pollution over the last two decades: A global perspective. *Science of The Total Environment*, *858*, 160064. https://doi.org/10.1016/j.scitotenv.2022.160064

Thapa, R. B., Murayama, Y., Ale, S. (2008). Kathmandu. *Cities*, *25*(1), 45–57. https://doi.org/10.1016/j.cities.2007.10.001

Tian, X., Cui, K., Sheu, H.-L., Hsieh, Y.-K., Yu, F. (2021). Effects of Rain and Snow on the Air Quality Index, PM2.5 Levels, and Dry Deposition Flux of PCDD/Fs. *Aerosol and Air Quality Research*, *21*(8), 210158. https://doi.org/10.4209/aaqr.210158

Trenchev, P., Dimitrova, M., Avetisyan, D. (2023). Determining background concentrations of major atmospheric pollutants using Sentinel-5P TROPOMI data. *Remote Sensing of Clouds and the Atmosphere XXVIII*, *12730*, 207–214. https://doi.org/10.1117/12.2679839

Vermote, E., Wolfe, R. (2021). *MODIS/Terra Surface Reflectance Daily L2G Global 1km and 500m SIN Grid V061* [dataset]. NASA EOSDIS Land Processes Distributed Active Archive Center. https://doi.org/10.5067/MODIS/MOD09GA.061

Vîrghileanu, M., Săvulescu, I., Mihai, B.-A., Nistor, C., Dobre, R. (2020). Nitrogen Dioxide (NO_2) Pollution Monitoring with Sentinel-5P Satellite Imagery over Europe during the Coronavirus Pandemic Outbreak. *Remote Sensing*, *12*(21), Article 21. https://doi.org/10.3390/rs12213575.

Vries, J. de, Voors, R., Ording, B., Dingjan, J., Veefkind, P., Ludewig, A., Kleipool, Q., Hoogeveen, R., Aben, I. (2016). TROPOMI on ESA's Sentinel 5p ready for launch and use. *Fourth International Conference on Remote Sensing and Geoinformation of the Environment (RSCy2016)*, *9688*, 86–97. https://doi.org/10.1117/12.2240839.

Wan, Z., Hook, S., Hulley, G. (2021). *MODIS/Terra Land Surface Temperature/Emissivity Daily L3 Global 1km SIN Grid V061* [dataset]. NASA EOSDIS Land Processes Distributed Active Archive Center. https://doi.org/10.5067/MODIS/MOD11A1.061.

WHO. (2022, December 19). *Ambient (outdoor) air pollution*. https://www.who.int/news-room/fact-sheets/detail/ambient-(outdoor)-air-quality-and-health.

WHO. (2023). *Air pollution*. Ambient (Outdoor) Air Pollution. https://www.who.int/health-topics/air-pollution.

Zheng, Z., Yang, Z., Wu, Z., Marinello, F. (2019). Spatial Variation of NO_2 and Its Impact Factors in China: An Application of Sentinel-5P Products. *Remote Sensing*, *11*(16), Article 16. https://doi.org/10.3390/rs11161939.